Electronic Supplementary Material (ESI) for Physical Chemistry Chemical Physics.

Supporting Information

Dynamic Pt-OH^-•H_2O-Ag Species Mediate Coupled Electron and Proton Transfer for Catalytic Hydride Reduction of 4-Nitrophenol at Confined Nanoscale Interface

Meng Ding, [1‡] Bing-Qian Shan, [1‡*] Bo Peng, [1] Jia-Feng Zhou, [1] Kun Zhang*[1,2,3]

[1] Shanghai Key Laboratory of Green Chemistry and Chemical Processes, College of Chemistry and Molecular Engineering, East China Normal University, Shanghai 200062, China;

[2] Laboratoire de chimie, Ecole Normale Supérieure de Lyon, Institut de Chimie de Lyon, Université de Lyon, 46 Allée d'italie, 69364 Lyon cedex 07, France;

[3] Shandong Provincial Key Laboratory of Chemical Energy Storage and Novel Cell Technology, School of Chemistry and Chemical Engineering, Liaocheng University, Liaocheng, 252059, Shandong, P. R. China.

[4] Institute of Eco-Chongming, Shanghai 202162, China.

* Correspondence: bqshan_ecnu@163.com, kzhang@chem.ecnu.edu.cn (K.Z.)

Table of Contents

Experiment section

Materials

Cetyltrimethylammonium tosylate (CTATos) was purchased from MERK. Triethanolamine ($TEAH_3$), tetraethylorthosilicate (TEOS) , (3-aminopropyl) trimethoxysilane (APTMS, 97%) were purchased from Aladdin., hydrochloric acid (HCI, 36%~38%), sodium hydroxide (NaOH, AR), sodium borohydride ($NaBH_4$, AR), , ethanol (EtOH, AR) and silver nitrate ($AgNO_3$, AR), Chloroplatinic acid (H_2PtCl_6, 37wt% Pt) were purchased from Sinopharm Chemical Reagent Co., Ltd. Potassium tetrachloroplatinate (K_2PdCl_6, 32.6 wt% Pd), Sodium borodeuteride ($NaBD_4$), Deuterium oxide (D_2O, 99% D) were achieved from Shanghai Macklin Biochemical.

Techniques

The X-ray diffraction (XRD) patterns were required using a Rigaku Ultima Discover X-Ray Diffractometer at a wavelength of Cu Kα (1.5405 Å). TEM analyses were performed by using a JEOL 2010F microscope equipped with a field-emission gun and operating at 200 kV. FTIR spectra were recorded on a Nicolet FTIR spectrometer (NEXUS 670) by diluting the sample with fine KBr powder and pressing into a pellet. Fluorescence was measured by using a FluorMax-4 fluorimeter (Horiba, Japan). Ultraviolet visible (UV–vis) spectroscopy was conducted with a Shimadzu UV-2700 UV–vis spectrophotometer and the $BaSO_4$ was used as reference. Fluorescence was measured by using a RF-6000 fluorimeter.

Synthesis of dendritic mesoporous silica nanospheres (DMSNs) supports

DMSNs were synthesized according to the literature report[1]. The DMSNs were treated by HCl(1M) and then functionalized by aminopropyl before grafting metal nanoparticles. In a typical process, 5 g of DMSNs, 8.4 mL of 1 M HCl and 200 mL of EtOH were added into a round-bottom flask, the mixture stirred at 60 °C for 1 h. The solid was dried at 80°C overnight after filtered and washed by deionized water and EtOH three times. Then, 3.250 g DMSNs washed by HCl, 5.655 g of APTMS and 130 mL EtOH were introduced into a round-bottom flask at 80°C for 12 h with stirring under reflux condition. The solution was filtered and washed by deionized water and EtOH. Then the solid was dried at 80°C overnight.

Synthesis of mesoporous silica nanopaticles loaded with different content of Pt-Ag Bimetals

In a 200 mL beaker, 0.7g of amino-functionalized DMSNs was suspended in 56 mL EtOH, subsequently added 1.1612 mL, 2.3222 ml, 4.6445 ml, 6.9668 ml of 7.72 mM $H_2PtCl_6{\cdot}6H_2O$ aqueous solution. After being stirred at room temperature for 12 h in dark, 7 mg, 14 mg, 28 mg, 42 mg $NaBH_4$ was added at once. The obtained product was filtered and washed repeatedly with deionized water and dried overnight at 80°C. The products were denoted as $Pt_{0.25}$@DMSNs, $Pt_{0.5}$@DMSNs, $Pt_{1.0}$@DMSNs, $Pt_{1.5}$@DMSNs. In a 200 mL beaker, 0.4g of different weight of Pt_x@DMSNs was suspended in 40 mL H_2O and treated by ultrasound for 30 minutes, and subsequently 1.295 mL, 1.11 ml, 0.74 ml, 0.37 ml of 50 mM $AgNO_3$ solution was added. After being stirred at room temperature for 3 h in dark, 49 mg, 42 mg, 28 mg, 14 mg $NaBH_4$ was added at once. Then the mixture was stirred unceasingly for 30 min. The obtained product was filtered and washed repeatedly with deionized H_2O and dried overnight at 80°C. The products were denoted as $Pt_{0.25}/Ag_{1.75}$@DMSNs, $Pt_{0.5}/Ag_{1.5}$@DMSNs, $Pt_{1.0}/Ag_{1.0}$@DMSNs, $Pt_{1.5}/Ag_{0.5}$@DMSNs. $Pt_{0.25}/Ag_{1.75}$-OH^-@DMSNs was prepared as according to the above method, except that after adding excess $NaBH_4$ and stirring 30 min, 14 mL of 1 M NaOH was added and stirred for 30 min. $Pt_{0.25}/Ag_xO_{1.75}$@DMSNs was prepared as according to the above method, except that excess $NaBH_4$ was instead of 14 mL of 1 M NaOH and stirred for 30 min. [2].

Reduction of 4-Nitrophenol

H_2O (2.5 mL), 4-NP (0.2 mL, 2.5 mM aqueous solution) and $NaBH_4$ (0.4 mL, 250 mM aqueous solution) were added into a quartz cuvette. The solution turned yellow. Subsequently, a certain amount (30 μL) of aqueous solution of catalyst (5 mg/mL) was added. As the reaction progressed, the bright yellow solution gradually faded. The reaction was scanned by UV-vis spectrum repeatedly from 500 nm to 250 nm over the whole course to record the changes. To test the effect of hydroxide content on the reaction activity, 2.5 mL of NaOH (0.01 M, 0.1 M, 1 M, 2 M aqueous solutions) was added instead of 2.5 mL H_2O. In the deuterium isotopic experiments, the reduction was conducted under the same conditions except for the use of $NaBD_4$ and/or D_2O.

The reaction kinetics can be modelled through the Langmuir–Hinshelwood mechanism as such:

$-d[4\text{-NP}]/dt = K\theta_{4\text{-NP}}\theta_{SB}$ (1)

where k is the intrinsic rate constant and $\theta_{4\text{-NP}}$ and θ_{SB} are the surface coverage of 4-NP and sodium borohydride (SB), respectively. Considering the surface adsorption/desorption equilibria for both 4-NP and $NaBH_4$, the rate law should take the following expression:

$-d[4\text{-NP}]/dt = K(S_0)^2K_{4\text{-NP}}[4\text{-NP}]K_{SB}[SB]/(1+K_{SB}[SB]+ K_{4\text{-NP}}[4\text{-NP}])^2$ (2)

where S_0 is the total active surface area of the catalysts as a constant and $K_{4\text{-NP}}$ and K_{SB} are the equilibrium constants for adsorption/desorption of 4-NP and SB, respectively. When $K_{SB}[SB] \gg K_{4\text{-NP}}[4\text{-NP}]$, the rate law can be further simplified to the following equation:

$-d[4\text{-NP}]/dt = K(S_0)^2K_{4\text{-NP}}[4\text{-NP}]K_{SB}[SB]/(1+K_{SB}[SB])^2$ (3)

When SB was in great excess with respect to the 4-NP (generally the molar ratio of SB/4-NP > 50), [SB] remained constant at its initial value, throughout the entire reaction process. Thus, this catalytic reaction follows pseudo-first-order kinetics as described by the following rate equations:

$-d[4\text{-NP}]/dt = K_{obs}[4\text{-NP}]$ (4)

where K_{obs} is the apparent pseudo-first-order rate constants.

In our cases, we performed kinetic measurements in the presence of excessive sodium borohydride with a molar ratio of SB/4-NP = 200 ([4-NP] = 0.2 mL, 2.5 mM, [SB] = 0.4 mL ,250mM) at nominally the same catalyst concentration (30 μL, 5 mg/mL). This answers our perfect linear fits of pseudo-first-order kinetics in Figure 1g, Figure 3b and 3c.

Large Scale Reduction of 4-NP.

To obtain more reduction products of 4-AP for spectroscopic measurements, large scale synthesis was carried out according to the literature[3]. First, 15 mg of 4-NP was dissolved in 3 mL of H_2O under magnetic stirring in reaction bottle, followed by addition of a 1 mL 5 mg/mL catalysts. Then, 30.0 mg of $NaBH_4$ was dissolved in 1 mL of H_2O and the solution was immediately added into the bottle. When the reaction completed. The completed reduction was confirmed by UV−vis absorption spectroscopic measurement, in which the peak of 4-NP at about 400 nm disappeared. Afterward, the solution was extracted with ethyl acetate three times and the products in the organic phase were collected and dried over anhydrous sodium sulfate ($NaSO_4$). Finally, the reduction products were obtained after evaporating the solvent under reduced pressure.

Experiment results

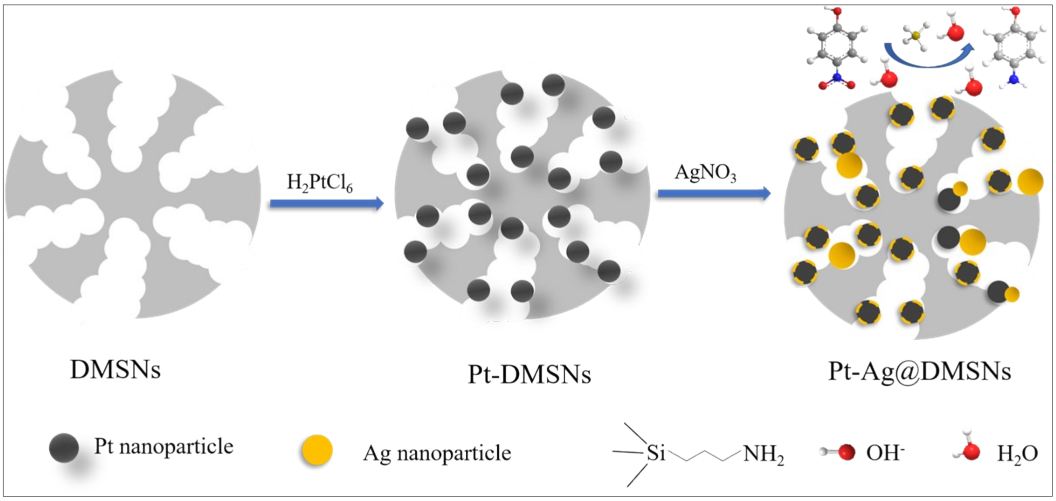

Figure S1. Schematic illustration of the synthesis procedure of Pt-Ag bimetallic supported

DMSNs catalysts (Pt_xAg_{2-x}@DMSNs).

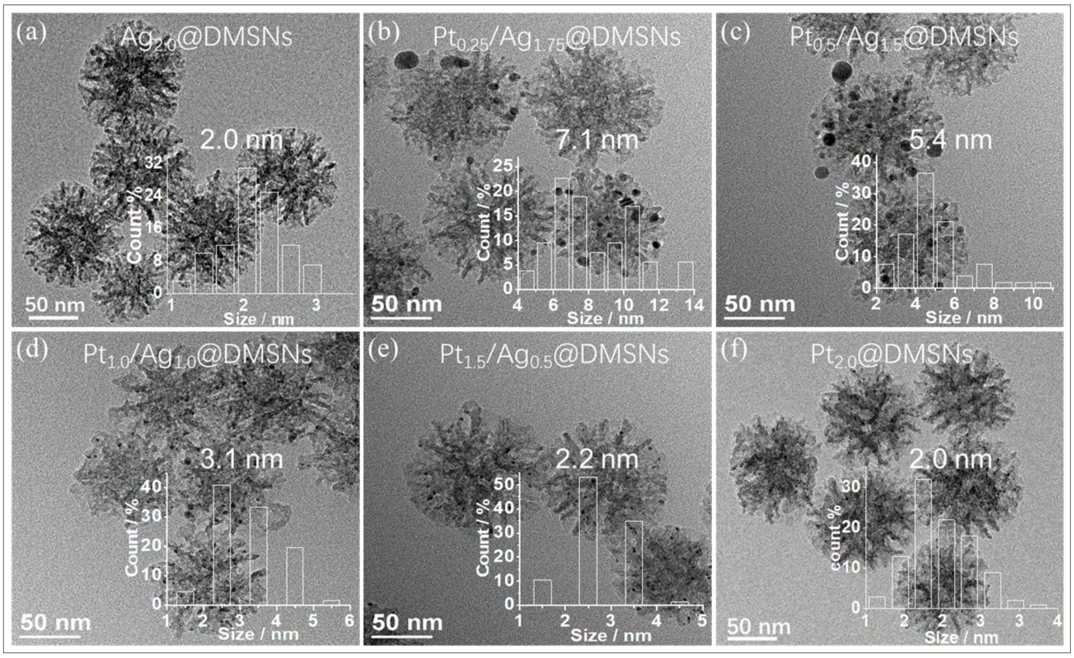

Figure S2. TEM images of Pt_xAg_{2-x}@DMSNs.

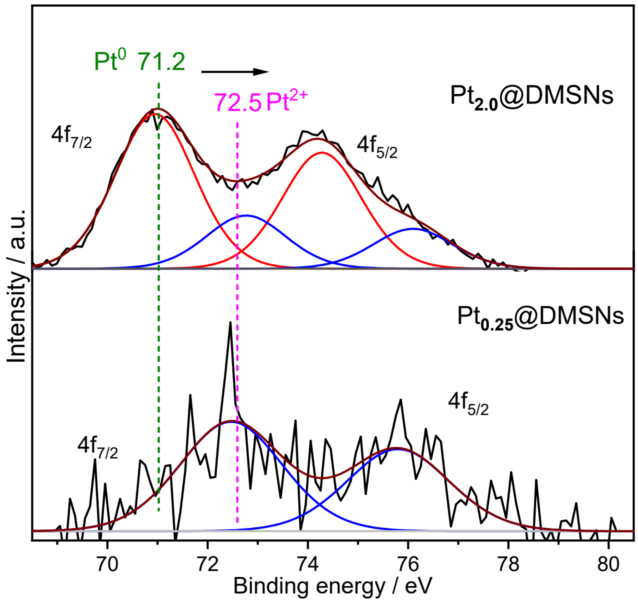

Figure S3. Pt 4f XPS spectra of $Pt_{2.0}$@DMSNs (up) and $Pt_{0.25}$@DMSNs (down).

Table S1. Surface compositions of Pt in catalysts determined by XPS.

Sample	**Pt position(eV)**		**Pt Component (%)**	
	Pt^0	Pt^{2+}	Pt^0	Pt^{2+}
$Pt_{0.25}Ag_{1.75}$@DMSN	/	73.1	/	100
$Pt_{0.25}$@DMSN	/	72.5	/	100
$Pt_{2.0}$@DMSN	71.2	72.7	74.5	25.5

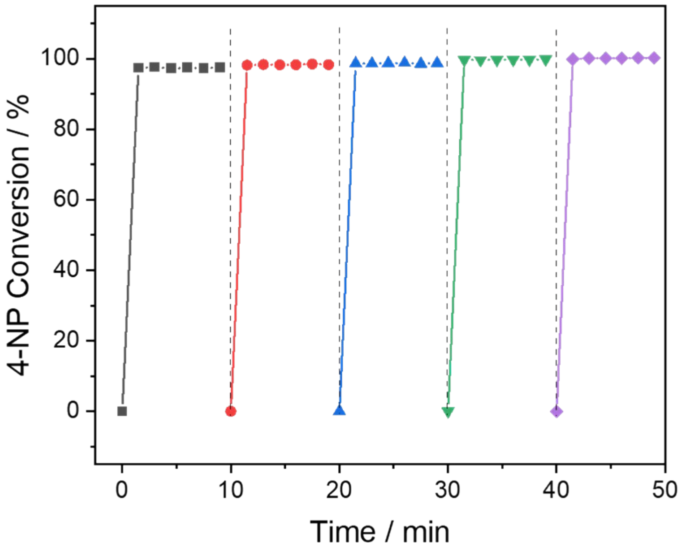

Figure S4. Stability test of the $Pt_{0.25}/Ag_{1.75}$@DMSNs catalyst for the reduction of 4-NP with $NaBH_4$.

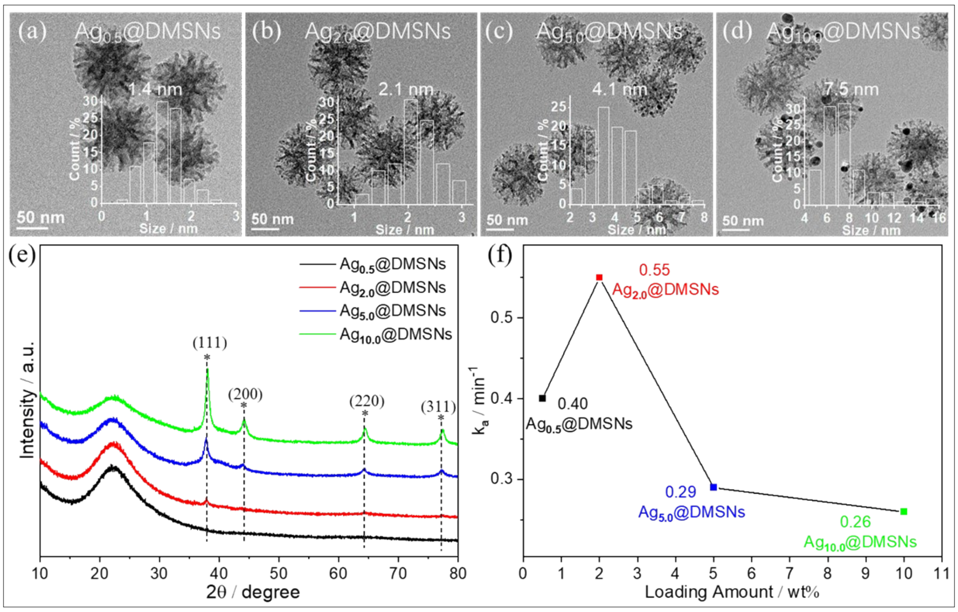

Figure S5. The TEM images (a-d), XRD (e) and catalytic reactivity (f) of Ag_x@DMSNs with different loading and particle size.

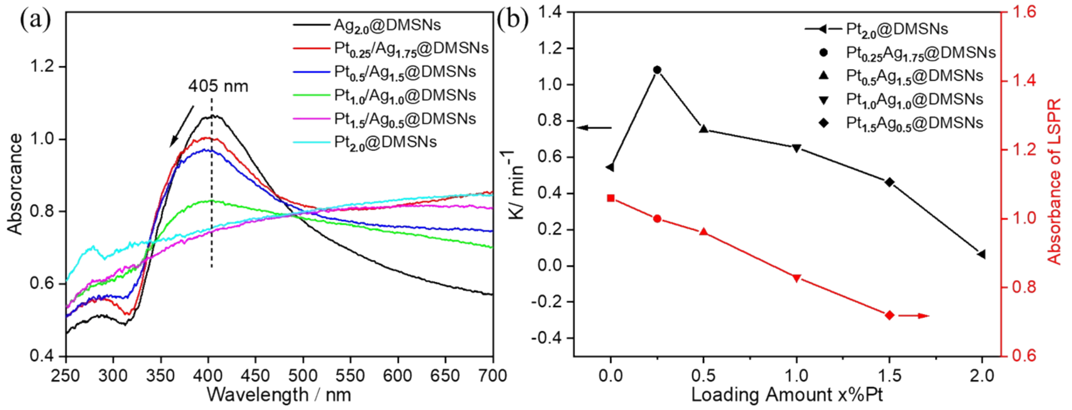

Figure S6. The ultraviolet−visible (UV−vis) absorption spectra (a). The catalytic reactivity and the strongest UV−vis absorbance peak (b) of bimetallic Pt_xAg_{2-x}@DMSNs catalysts.

Table S2. Surface compositions of Ag in catalysts determined by XPS.

Sample	Ag position(eV)		Ag Component (%)	
	Ag^0	Ag^+	Ag^0	Ag^+
$Ag_{2.0}$@DMSN	368.1	369.7	91.3	8.7
$Pt_{0.25}Ag_{1.75}$@DMSN	368.5	370.6	96.3	3.7

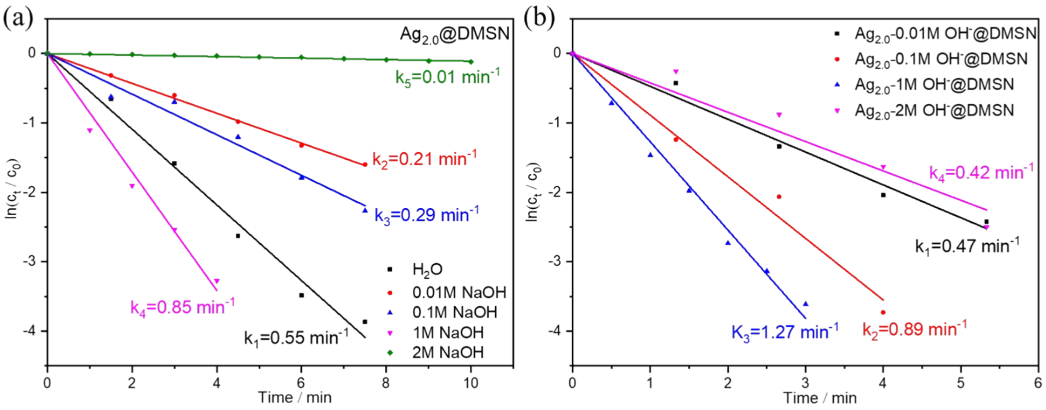

Figure S7. Plots of ln (C_t/C_0) against the reaction time for the reduction of 4-NP over monometal $Ag_{2.0}$@DMSNs catalysts: (a) Different concentrations of sodium hydroxide are directly introduced into the reaction system, and (b) $Ag_{2.0}$@DMSNs catalysts were pre-impregnated with different concentrations of sodium hydroxide.

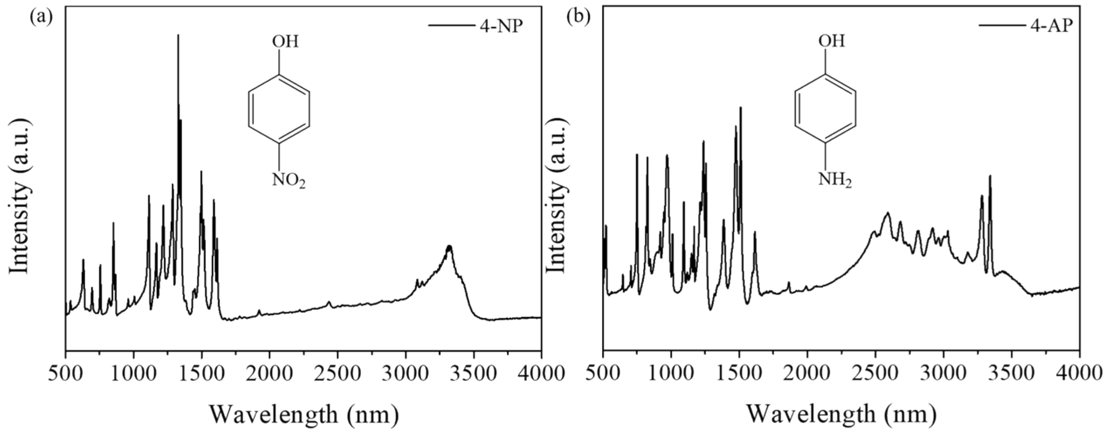

Figure S8. FTIR spectrum of commercial 4-AP and 4-NP.

Table S3. Comparison of recent reports on Ag-based catalysts catalyzed reduction of 4-NP by $NaBH_4$.

Catalyst	Catalyst used (mg)	K^a (10^{-3} s^{-1})	K/M^b (s^{-1} g^{-1})	Ref.
Ag–Fe_2O_3	2.00	4.90	2.45	[4]
Fe_3O_4@SiO_2–Ag	1.00	7.67	7.67	[5]
Ag@hm-SiO_2	2.00	18.00	9.00	[6]
AgNPs/PD/PANFP	0.14	2.28	16.31	[7]
SiO_2@Ag-2	0.50	9.32	18.64	[8]
$Ag_{2.4\%}$Ni@SBA-16C	0.40	37.90	94.80	[9]
Pt@Ag NPs	0.05	5.92	118.40	[10]
2.0%Ag-OH^-@DMSNs	0.15	21.17	141.13	[2]
Ag-OMS-C	0.20	30.00	150.00	[11]
Ag@LTA	0.15	22.67	151.13	[12]
$Pt_{0.25}Ag_{1.75}$@DMSNs	0.15	18.05	120.33	This work

Reference

1. Zhang, K.; Xu, L. L.; Jiang, J. G.; Calin, N.; Lam, K. F.; Zhang, S. J.; Wu, H. H.; Wu, G. D.; Albela, B.; Bonneviot, L.; Wu, P., Facile large-scale synthesis of monodisperse mesoporous silica nanospheres with tunable pore structure. *J. Am. Chem. Soc.* **2013,** *135* (7), 2427-30.

2. Hu, X.-D.; Shan, B.-Q.; Tao, R.; Yang, T.-Q.; Zhang, K., Interfacial Hydroxyl Promotes the Reduction of 4-Nitrophenol by Ag-based Catalysts Confined in Dendritic Mesoporous Silica Nanospheres. *J. Phys. Chem. C* **2021,** *125* (4), 2446-2453.

3. Zhao, Y.; Li, R.; Jiang, P.; Zhang, K.; Dong, Y.; Xie, W., Mechanistic Study of Catalytic Hydride Reduction of −NO2 to −NH2 Using Isotopic Solvent and Reducer: The Real Hydrogen Source. *J. Phys. Chem. C* **2019,** *123* (25), 15582-15588.

4. Liu, S.; Chen, Y.; Dong, L., Ag–Fe2O3nanocomposites with enhanced catalytic activity for reduction of 4-nitrophenol. *Mater. Res. Express* **2016,** *3* (7), 075024.

5. Chi, Y.; Yuan, Q.; Li, Y.; Tu, J.; Zhao, L.; Li, N.; Li, X., Synthesis of Fe3O4@SiO2–Ag magnetic nanocomposite based on small-sized and highly dispersed silver nanoparticles for catalytic reduction of 4-nitrophenol. *J. Colloid Interface Sci.* **2012,** *383* (1), 96-102.

6. Li, W.; Ge, X.; Zhang, H.; Ding, Q.; Ding, H.; Zhang, Y.; Wang, G.; Zhang, H.; Zhao, H.,

Hollow mesoporous SiO2 sphere nanoarchitectures with encapsulated silver nanoparticles for catalytic reduction of 4-nitrophenol. *Inorg. Chem. Front.* **2016,** *3* (5), 663-670.

7. Lu, S.; Yu, J.; Cheng, Y.; Wang, Q.; Barras, A.; Xu, W.; Szunerits, S.; Cornu, D.; Boukherroub, R., Preparation of silver nanoparticles/polydopamine functionalized polyacrylonitrile fiber paper and its catalytic activity for the reduction 4-nitrophenol. *Appl. Surf. Sci.* **2017,** *411*, 163-169.
8. Tzounis, L.; Contreras-Caceres, R.; Schellkopf, L.; Jehnichen, D.; Fischer, D.; Cai, C.; Uhlmann, P.; Stamm, M., Controlled growth of Ag nanoparticles decorated onto the surface of SiO2 spheres: a nanohybrid system with combined SERS and catalytic properties. *RSC Adv.* **2014,** *4* (34), 17846-17855.
9. Budi, C. S.; Deka, J. R.; Saikia, D.; Kao, H.-M.; Yang, Y.-C., Ultrafine bimetallic Ag-doped Ni nanoparticles embedded in cage-type mesoporous silica SBA-16 as superior catalysts for conversion of toxic nitroaromatic compounds. *J. Hazard. Mater.* **2020,** *384*, 121270.
10. Lv, Z.-S.; Zhu, X.-Y.; Meng, H.-B.; Feng, J.-J.; Wang, A.-J., One-pot synthesis of highly branched Pt@Ag core-shell nanoparticles as a recyclable catalyst with dramatically boosting the catalytic performance for 4-nitrophenol reduction. *J. Colloid Interface Sci.* **2019,** *538*, 349-356.
11. Fan, H.-T.; Liu, X.-G.; Xing, X.-J.; Li, B.; Wang, K.; Chen, S.-T.; Wu, Z.; Qiu, D.-F., Ordered mesoporous silica cubic particles decorated with silver nanoparticles: a highly active and recyclable heterogeneous catalyst for the reduction of 4-nitrophenol. *Dalton Trans.* **2019,** *48* (8), 2692-2700.
12. Shan, B. Q.; Zhou, J. F.; Ding, M.; Hu, X. D.; Zhang, K., Surface Electronic State Mediates Proton Transfer at Metal Nanoscale Interface for Catalytic Hydride Reduction of $-NO_2$ to $-NH_2$. *Phys. Chem. Chem. Phys.* **2021**, 23, 12950-12957.